Dispersion management for nonlinearity mitigation in two-span 28 GBaud QPSK phase-sensitive amplifier links

Research Article | Vol. 25, No. 12 | 12 Jun 2017 | OPTICS EXPRESS 13163
Optics EXPRESS

Dispersion management for nonlinearity mitigation in two-span 28 GBaud QPSK phase-sensitive amplifier links

EGON ASTRA,[1,*] SAMUEL L. I. OLSSON,[2,3] HENRIK ELIASSON,[2] AND PETER A. ANDREKSON[1,2]

[1] *Thomas Johann Seebeck Department of Electronics, Tallinn University of Technology, Tallinn, Estonia*
[2] *Department of Microtechnology and Nanoscience, Photonics Laboratory, Chalmers University of Technology, Göteborg, Sweden*
[3] *Now at: Nokia Bell Labs, 791 Holmdel Road, Holmdel, NJ 07733, USA*
[*] *egon.astra@ttu.ee*

Abstract: We present an investigation of dispersion map optimization for two-span single-channel 28 GBaud QPSK transmission systems with phase-sensitive amplifiers (PSAs). In experiments, when the PSA link is operated in a highly nonlinear regime, a 1.4 dB error vector magnitude (EVM) improvement is achieved compared to a one-span optimized dispersion map link due to improved nonlinearity mitigation. The two-span optimized dispersion map of a PSA link differs from the optimized dispersion map of a dispersion managed phase-insensitive amplifier (PIA) link. Simulations show that the performance of the two-span dispersion map optimized PSA link does not improve by residual dispersion optimization. Further, by using the two-span optimized dispersion maps repeatedly in a long-haul PSA link instead of one-span optimized maps, the maximum transmission reach can be improved 1.5 times.

OCIS codes: (060.2320) Fiber optics amplifiers and oscillators; (070.4340) Nonlinear optical signal processing; (190.4380) Nonlinear optics, four-wave mixing.

References and links

1. Z. Tong, C. Lundström, P. A. Andrekson, C. J. McKinstrie, M. Karlsson, D. J. Blessing, E. Tipsuwannakul, B. J. Puttnam, H. Toda, and L. Grüner-Nielsen, "Towards ultrasensitive optical links enabled by low-noise phase-sensitive amplifiers," Nat. Photonics **5**(7), 430–436 (2011).
2. S. L. I. Olsson, B. Corcoran, C. Lundström, T. A. Eriksson, M. Karlsson, and P. A. Andrekson, "Phase-Sensitive Amplified Transmission Links for Improved Sensitivity and Nonlinearity Tolerance," J. Lightwave Technol. **33**(3), 710–721 (2015).
3. S. L. I. Olsson, C. Lundström, M. Karlsson, and P. A. Andrekson, "Long-Haul (3465 km) Transmission of a 10 GBd QPSK Signal with Low Noise Phase-Sensitive In-Line Amplification," in Proc. European Conference on Optical Communications (ECOC, 2014), paper PD.2.2.
4. X. Liu, A. R. Chraplyvy, P. J. Winzer, R. W. Tkach, and S. Chandrasekhar, "Phase-Conjugated Twin Waves for Communication Beyond the Kerr Nonlinearity Limit," Nat. Photonics **7**(7), 560–568 (2013).
5. W. Forysiak, J. H. B. Nijhof, and N. J. Doran, "Dispersion Managed Solitons: The Key to Terabit Per Second Optical Fiber Communication Systems," Opt. Photon. News **11**(5), 35–39 (2000).
6. C. Peucheret, N. Hanik, R. Freund, L. Molle, and P. Jeppesen, "Optimization of pre- and post-dispersion compensation schemes for 10-Gbits/s NRZ links using standard and dispersion compensating fibers," Photon. Technol. Lett. **12**(8), 992–994 (2000).
7. Y. Frignac and S. Bigo, "Numerical optimization of residual dispersion in dispersion-managed systems at 40 Gbit/s," in Proc. Optical Fiber Communications Conference and Exhibition (OFC, 2000), paper TuD3-1.
8. M. Malach, C.-A. Bunge, and K. Petermann, "Fibre-Independent Optimum Dispersion Mapping for SPM and XPM Suppression in 10 Gbit/s WDM NRZ Optical Transmission Systems," in Proc. European Conference on Optical Communications (ECOC, 2006), paper We3.P.130.
9. J. K. Fischer, C.-A. Bunge, and K. Petermann, "Equivalent Single-Span Model for Dispersion-Managed Fiber-Optic Transmission Systems," J. Lightwave Technol. **27**(16), 3425–3432 (2009).
10. A. Cartaxo, N. Costa, and D. Fonseca, "Analysis of optimum dispersion maps for DQPSK systems," in Proc. International Conference on Transparent Optical Networks (ICTON, 2010), paper Mo.D1.1.
11. Y. Frignac and P. Ramantanis, "Average Optical Phase Shift as an Indicator of the Dispersion Management Optimization in PSK-Modulated Transmission Systems," Photon. Technol. Lett. **22**(20), 1488–1490 (2010).

#290195 https://doi.org/10.1364/OE.25.013163
Journal © 2017 Received 8 Mar 2017; revised 26 Apr 2017; accepted 27 Apr 2017; published 31 May 2017
Corrected: 17 October 2017

Optics EXPRESS

12. B. Corcoran, S. L. I. Olsson, C. Lundström, M. Karlsson, and P. A. Andrekson, "Mitigation of Nonlinear Impairments on QPSK Data in Phase-Sensitive Amplified Links," in Proc. European Conference on Optical Communications (ECOC, 2013), paper We.3.A.1.
13. H. Eliasson, S. L. I. Olsson, M. Karlsson, and P. A. Andrekson, "Mitigation of nonlinear distortion in hybrid Raman/phase-sensitive amplifier links," Opt. Express **24**(2), 888–900 (2016).
14. E. Astra, S. L. I. Olsson, H. Eliasson, T. Laadung, and P. A. Andrekson, "Dispersion Map Optimization for Nonlinearity Mitigation in Two-Span Phase-Sensitive Amplifier Links," in Proc. European Conference on Optical Communications (ECOC, 2016), paper Th.1.A.3.
15. S. L. I. Olsson, B. Corcoran, C. Lundström, E. Tipsuwannakul, S. Sygletos, A. D. Ellis, Z. Tong, M. Karlsson, and P. A. Andrekson , "Injection locking-based pump recovery for phase-sensitive amplified links," Opt. Express **21**(12), 14512-14529 (2013).
16. H. Eliasson, S. L. I. Olsson. M. Karlsson, and P. A. Andrekson, "Comparison between coherent superposition in DSP and PSA for mitigation of nonlinearities in a single-span link," in Proc. European Conference on Optical Communications (ECOC, 2014), paper Mo.3.5.2.

1. Introduction

Phase-sensitive amplifiers (PSAs) are implemented by making use of the four-wave mixing (FWM) process of signal, idler and pump waves in a nonlinear medium e.g. a highly nonlinear fiber (HNLF). If PSAs are used as in-line amplifiers in a fiber-optic communication link instead of phase-insensitive amplifiers (PIAs), a signal quality improvement is possible due to the PSA's ability to provide simultaneously low-noise amplification and nonlinearity mitigation [1–3].

In single-channel two-mode PSA-amplified links, the signal wave is co-propagated with an idler wave that is a conjugated copy of the signal wave, located at a different wavelength. The nonlinearity mitigation in such links is the result of correlated nonlinear distortion on signal and idler and the all-optical coherent superposition (CS) of signal and the conjugate of the idler in the PSA [2]. A similar approach for nonlinearity mitigation is the phase-conjugated twin waves (PCTW) scheme, where a phase-conjugated copy of the signal is co-propagated on the orthogonal polarization and the CS is performed electronically after coherent detection in digital signal processing (DSP) [4].

It is well known that the link dispersion map plays an important role in the interaction of group velocity dispersion (GVD) and nonlinear effects [5, 6]. It has been found that for non-return-to-zero (NRZ) and return-to-zero on-off-keying (RZ-OOK) modulation formats, non-zero residual dispersion per span can reduce the impact of nonlinear impairments [7–9] and the same holds for quadrature phase-shift keying (QPSK) [10]. It has also been shown that the optimization of link dispersion map minimizes the average nonlinear phase-shift introduced by the interplay of GVD and nonlinearities [11].

The optimum amount of dispersion pre- and post-compensation for PSA-amplified links has been thoroughly investigated for the single-span scenario [2, 12] and such a single-span optimized dispersion map has been used in multi-span PSA links [3, 13]. Also the temporal walk-off induced by different dispersion values between signal and idler waves at their wavelengths in the standard single mode fiber (SSMF) were compensated for before coherent interaction of signal and idler in the PSA. Thus, only fully dispersion compensated spans in PSA links has been studied to date [1–3, 12–14].

In [14] we showed numerically and experimentally that using the single-span optimized dispersion map for both spans in a two-span PSA link is not optimal and allowing different span dispersion maps in the two spans can improve the nonlinearity mitigation performance. In this paper we expand our results on dispersion map optimization of two-span single-channel 28 GBaud QPSK PSA links by including more details, investigate the effects of residual dispersion in a simulation study and compare the found optimal dispersion map configurations in long-haul PSA link simulations.

Optics EXPRESS

2. Numerical investigation

2.1. Two-span simulation model

The simulation model of the two-span PSA link in Fig. 1 consists of a transmitter, two in-line dispersion compensated transmission spans amplified by PSAs and receiver DSP. In the transmitter, a single-channel and single-polarization 28 GBaud QPSK signal was generated and separated into signal and idler channels. In the idler channel, the signal was conjugated to generate the idler, fulfilling $I_1 = S_1^*$. The launch powers P_{in} were set equal for the signal and idler at the span input for both spans. The effects of polarization, higher-order dispersion and laser phase noise were neglected. The dispersion pre- and post-compensation performed in the dispersion compensating modules (DCMs) was linear and lossless. Also amplifier noise was neglected in the two-span simulations, assuming that signal-noise interaction is negligible. These simplifications were made to highlight the impact of the dispersion map on the efficiency of the mitigation of self-phase modulation (SPM) induced nonlinear distortion.

Both spans were dispersion pre- and post-compensated in DCMs before and after the 80 km of SSMF. The dispersion pre-compensation values $D_{\text{pre},1}$ of span 1 and $D_{\text{pre},2}$ of span 2 show the percentage of dispersion pre-compensation applied in the DCMs before the SSMF. Each span was fully dispersion compensated, but the span dispersion maps were chosen independently. The dispersion post-compensation values for the DCMs after the SSMFs can be found by subtracting the span pre-compensation values from 100%. The SSMF parameters were loss $\alpha = 0.2$ dB/km, dispersion parameter $D = 17$ ps/nm/km and nonlinear coefficient $\gamma = 1.27$ W^{-1}km^{-1}. The light propagation in SSMF was modelled using a split-step Fourier method (SSFM) solution of the nonlinear Schrödinger equation (NLSE). Two separate single-polarization NLSE solvers with the same propagation parameters were used for signal and idler propagation, as the signal and idler were separated by 8 nm (signal 1549.74 nm and idler 1558.60 nm) in experiment. Therefore it was assumed that the nonlinear cross-talk between signal and idler waves in the SSMF was negligible compared to SPM.

The PSA gain was set to compensate for the transmission span loss. The two-mode PSA amplification process was modeled as in [2]. It was assumed that the PSA was working in high-gain regime and therefore a simplified PSA model was used. In the first PSA, S_1' from the signal channel and I_1' from the idler channel were separated and conjugated using the conjugate operator. After conjugation the constellations were aligned by introducing a necessary phase rotation in the constellation alignment (CA) module, so that the optical power was maximized

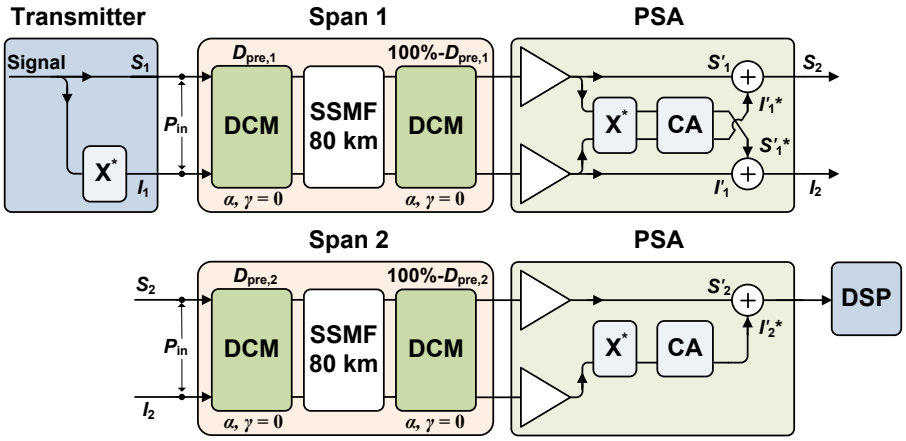

Fig. 1. Simulation model of the two-span PSA link. Acronyms are explained in the text.

Optics EXPRESS

after the coherent addition of signal and idler waves. After CS the signal channel output is given by $S_2 = S_1' + I_1'^*$ and for the idler channel $I_2 = S_1'^* + I_1'$. In the second PSA, after span 2, the idler channel output was not used in the DSP input and therefore the coherent addition in the idler channel was dropped for simplicity. Conventional receiver DSP was used for QPSK signal post-processing consisting of a linear channel equalizer, phase recovery and error vector magnitude (EVM) value calculation with hard decision thresholds.

2.2. Simulation results

The EVM value as a function of dispersion pre-compensation values for span 1 (y-axis) and span 2 (x-axis) at 12 dBm signal launch power, meaning 15 dBm total power of signal and idler, are shown in Fig. 2(a) for a PSA amplified link. The dispersion compensation ratio between pre- and post-compensation was changed from 0% to 100% in steps of 5% in each span, resulting in 441 different dispersion map configurations. Figure 2(a) shows that there exists two optima that have different amounts of applied dispersion pre-compensation values for both spans, 5% for span 1 and 35% for span 2 (5%, 35%) with EVM = -11.2 dB or the other way around (35%, 5%) with EVM = -11.1 dB. These optima are positioned symmetrically around the diagonal. The one span dispersion map optimized PSA link in two-span configuration with 15 % dispersion pre-compensation value for both spans (15%, 15%) has EVM = -8.9 dB. The EVM improvement using the two-span optimized dispersion map (5%, 35%) PSA link compared to the one span dispersion map optimized PSA link (15%, 15%) is thus 2.3 dB. These relatively high launch powers in simulations were needed to determine whether it is possible to observe and confirm any nonlinearity mitigation improvement effects experimentally that were predicted by simulations.

The two-span dispersion map optimization simulations were also compared and evaluated with a more realistic propagation model (not presented in this paper), where the third-order dispersion (TOD) effects were included, meaning that the dispersion value for signal and idler was different $D_s \neq D_i$. At signal wavelength 1550 nm the dispersion value D_s = 17 ps/nm/km and at idler wavelength 1558 nm the dispersion value D_i = 17.5 ps/nm/km were applied. Also ideal dispersion compensation and time delay alignment for signal and idler were assumed. No

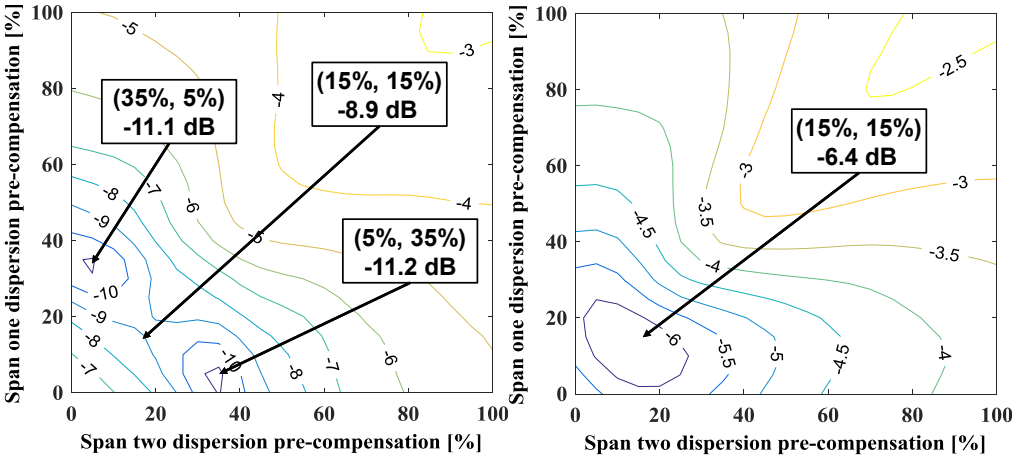

Fig. 2. Simulation results of EVM at 12 dBm signal launch power, meaning 15 dBm total power of signal and idler, of the two-span (a) PSA amplified and (b) PIA amplified link; The y- and x-axis show the percentages of applied dispersion pre-compensation in span 1 and span 2 respectively.

Optics EXPRESS

significant differences in the simulation results were observed when third-order dispersion was included. For simplicity and to achieve a better understanding of the fundamental role of the dispersion management in two-span PSA amplified systems, the effects of higher-order dispersion were not included in the simulation results presented here.

In Fig. 2(b) the EVM as a function of the dispersion pre-compensation values for span 1 and span 2 at 12 dBm signal launch power are shown for a two-span PIA amplified link. The PIA link simulation model is similar to the PSA link model shown in Fig. 1 with the difference that the idler and its channel are not present in the model. Instead of PSA module is phase-insensitive amplifier that amplifies only signal wave. Therefore only signal is transmitted and in-line amplified. The optimal dispersion pre-compensation values for the PIA link are 15% for span 1 and 15% for span 2 (15%, 15%) with EVM value of -6.4 dB. The overall performance in terms of nonlinearity mitigation of a dispersion managed two-span PIA link can be improved by 2.5 dB by making use of PSA amplification and 4.8 dB in total, if PSAs and two-span dispersion map optimization are applied for improved nonlinearity mitigation. It is however clear from the comparison, that the optimized dispersion map for the PSA link is different from the optimized dispersion map for the PIA link and the mechanism for mitigating nonlinear distortion by the right choice of dispersion map for the PIA links is different than for the PSA link.

In Figs. 3(a) and 3(b) the optimal dispersion pre-compensation values of a two-span PSA link are shown as a function of loss parameter α at 12 dBm signal launch power and as a function of signal launch power at loss α = 0.2 dB/km with the dispersion parameter D = 17 ps/nm/km and nonlinear coefficient γ = 1.27 $W^{-1}km^{-1}$. The dispersion compensation ratio in these simulations was also swept with a step size of 5%. Figure 3(a) shows that the optimum dispersion map configuration varies significantly with the loss parameter α. Figure 3(b) shows, that the optimum dispersion map does not depend on signal launch power. Simulations were also performed with sweeped dispersion parameter D in the range from 4 to 34 ps/nm/km and the nonlinear coefficient γ from 0.1 to 2.3 $W^{-1}km^{-1}$ at 12 dBm signal launch power with loss α = 0.2 dB/km, but no significant change in the two-span optimum dispersion map configuration was noticed. It follows that the dispersion length L_D and nonlinear length L_{NL} do not have a strong influence compared to the effective length L_{eff} of the SSMF on the optimal dispersion map configuration at least for

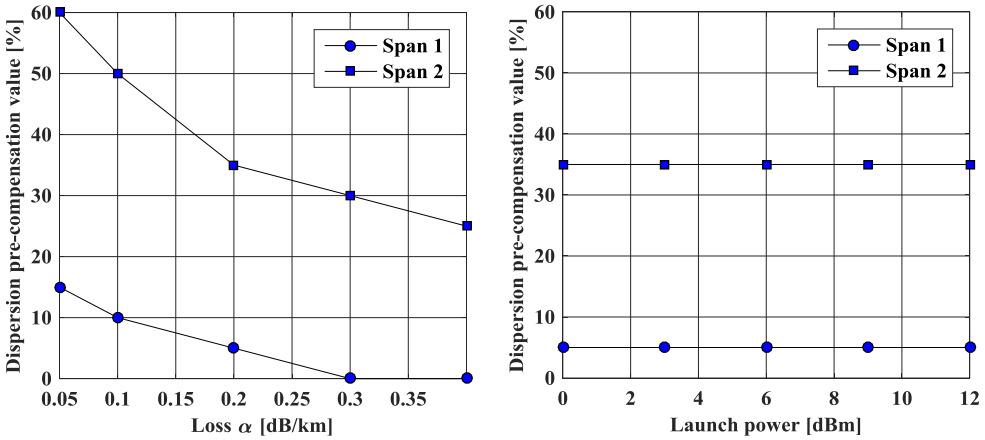

Fig. 3. Simulation results of a two-span PSA amplified link showing optimal dispersion pre-compensation values for both spans as a function of (a) loss α at 12 dBm launch power and (b) signal launch power at loss α = 0.2 dB/km.

Optics EXPRESS

the modulation format and symbol rate studied here.

Simulations with similar parameters and parameter sweep-ranges were also performed for a dispersion managed two-span PIA link. The results from these simulations (not presented here) show that the optimum dispersion map configuration for a two-span PIA link is not significantly dependent on the effective length L_{eff} of the SSMF as it was observed for the PSA link. Also no significant change by dispersion length L_{D} and nonlinear length L_{NL} on the optimum dispersion map configuration of the SSMF for the two-span PIA link was noticed.

3. Experimental investigation

3.1. Experimental setup

Figure 4 shows the setup used for the experimental investigation. A 28 GBaud QPSK signal was generated at 1549.74 nm and combined with a high-power continuous wave (CW) pump at 1554.16 nm using a wavelength division multiplexing (WDM) coupler. Before the signal and pump were combined and launched into a fiber optical parametric amplifier (FOPA), the copier, the signal and pump polarizations were controlled using polarization controllers (PCs). In the copier, a phase-conjugated copy of the signal, the idler, at 1558.60 nm was generated. After the copier, the signal and idler were separated from the pump for power balancing using an optical processor (OP), dispersion pre-compensation using a tunable dispersion compensating module (TDCM1) and amplification using an erbium doped fiber amplifier (EDFA). After power adjustment using variable optical attenuators (VOAs), the signal, idler and pump were recombined and launched into span 1 consisting of 80 km of SSMF.

After span 1, the signal, idler and pump were separated from each other. A variable delay line was used to compensate for the different propagation delays experienced by the signal and idler in span 1. A VOA in the idler path was used for equalizing the signal and idler powers at the input of the PSA. The three PCs were used to align the signal, idler and pump state-of-polarizations (SOPs) before the PSA. The signal and idler were combined and subsequently dispersion post-compensated in TDCM2. The received signal and idler powers were kept constant using a VOA

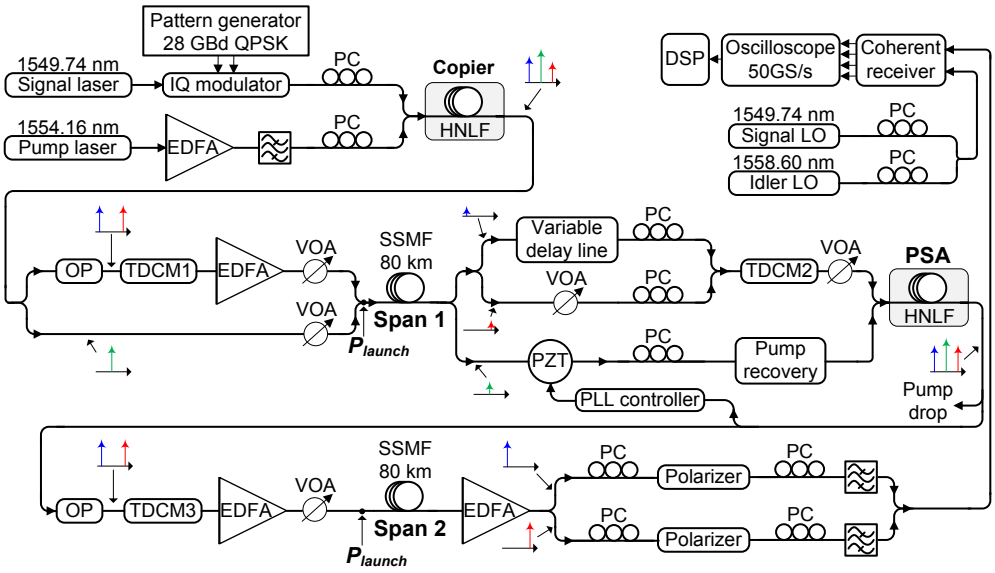

Fig. 4. The experimental setup used for two-span PSA link measurements. Acronyms are explained in the text.

Optics EXPRESS

to ensure a fixed OSNR after the PSA. A piezoelectric transducer (PZT) and a phase-locked loop (PLL) controller was used to dynamically adjust the relative phase between signal, idler and pump so that the PSA gain was maximized. A pump recovery stage was used to regenerate and amplify the pump using optical injection-locking [15]. The pump, signal and idler were recombined and launched into the PSA. The PSA on-off gain was 20 dB.

After the PSA, the pump was dropped and the signal and idler were passed through an OP for power adjustments, so that the signal and idler powers launched into span 2 were equal. TDCM3 was used for dispersion pre-compensation of span 2 and an EDFA followed by a VOA was used for setting the signal and idler powers launched into span 2, that consisted of 80 km SSMF. The launch powers P_{launch} of signal and idler were set equal before both spans. After span 2, the signal and idler were amplified using an EDFA and split into two separated paths. Polarization controllers (PCs), polarizers and filters were used before the receiver for the removal of non-co-polarized amplifier noise and to adjust the SOPs of signal and idler so that they were orthogonal. After recombining the signal and idler, they were coherently detected using a dual-polarization hybrid in the receiver and sampled at 50 GS/s before being processed in DSP. Span 2 dispersion post-compensation and coherent superposition was performed electronically in DSP. It has been demonstrated that SPM mitigation in a single-span link is performed equally well all-optically using a PSA and electronically in DSP [16].

3.2. Experimental results

The two-span optimized (5%, 35%) and one-span optimized (15%, 15%) dispersion map configurations were compared. It should be noted that the used dispersion maps were not optimized experimentally and the selection was based on the simulation results, limited in accuracy mainly by the dispersion compensation step size of 5% and the chosen loss parameter α. In Fig. 5(a) the experimentally measured EVM values as a function of signal launch power for the two different dispersion map scenarios are shown. The two-span optimized dispersion map configuration (5%, 35%) outperforms the one-span optimized dispersion map configuration (15%, 15%) case. The highest EVM performance improvement, 1.4 dB, is observed at 13 dBm signal launch power. This lower EVM improvement compared to the simulation results, where an EVM improvement of 2.3 dB was predicted, is attributed to amplifier noise that was present in the system and the fact that the optimum dispersion map was not experimentally optimized.

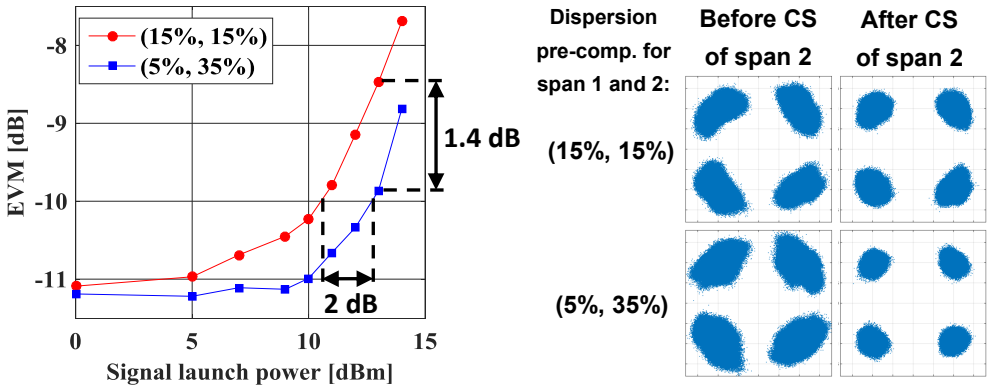

Fig. 5. Measured (a) EVM versus signal launch power for two dispersion map configurations, (b) constellation diagrams showing the signal before and after CS of span 2 at 13 dBm signal launch power.

Optics EXPRESS

In Fig. 5(a), we also see that the two-span optimized dispersion map configuration shows 2 dB higher launch power tolerance at an EVM of -10 dB. The calculated nonlinear phase shift is 1.1 radians at 13 dBm signal launch power.

Figure 5(b) shows constellation diagrams for the two dispersion map scenarios before and after CS of span 2 at 13 dBm launch power. Before CS of span 2, the constellations are more severely distorted for the (5%, 35%) dispersion map configuration than for the (15%, 15%) dispersion map configuration. However the opposite is true after CS of span 2, where the (5%, 35%) dispersion map configuration shows less distorted constellations. This confirms the simulation results and shows that the optimal dispersion map does not minimize the interplay between GVD and SPM effects which is the case in ordinary dispersion managed single-channel QPSK PIA transmission links [11]. However, in the two-span dispersion map optimized PSA link, the nonlinear distortions on the signal and idler are correlated to a higher degree compared to the one-span dispersion map optimized case, resulting in a more efficient mitigation of nonlinear distortions by the CS of span 2.

4. The impact of residual dispersion in PSA

Simulations of one-span and two-span PSA links were conducted where, in addition, residual dispersion per span was allowed to be non-zero. The same simulation model as illustrated in Fig. 1 was used, but with the difference that the dispersion post-compensation was performed to under- or overcompensate the dispersion by given values. In the one-span PSA link, the DSP processing and EVM calculation was done after the first PSA. Figure 6 shows EVM performance as a function of total dispersion compensation and dispersion pre-compensation for a one-span PSA link. Dispersion compensation values were swept with a step size of 5%. Figure 6 shows that without residual dispersion the best EVM performance of -11.8 dB is achieved at a dispersion pre-compensation value of 15%. However, the EVM can be enhanced 0.8 dB by setting the dispersion pre-compensation value to 20% and introducing 10% residual dispersion, meaning 90% total dispersion compensation before CS in a one-span PSA link.

Figures 7(a) and 7(b) show the EVM performance assuming that the total dispersion compensation value in both spans of a two-span PSA link are varied. In Fig. 7(a) the one-span optimized dispersion map with 15% dispersion pre-compensation applied in both spans (15%, 15%) is

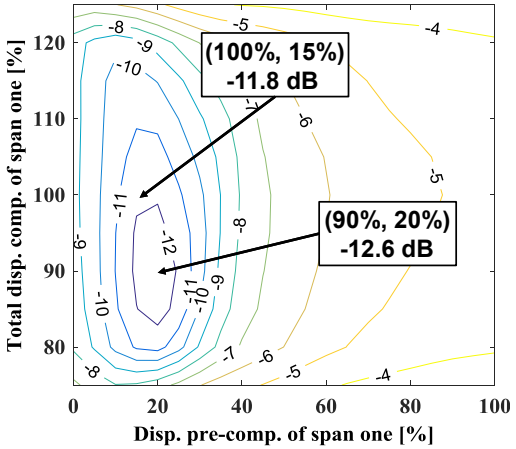

Fig. 6. Simulation results showing EVM of a one-span PSA amplified link at 12 dBm signal launch power where the span total dispersion compensation percentage is indicated on the y-axis and dispersion pre-compensation values on the x-axis.

Optics EXPRESS

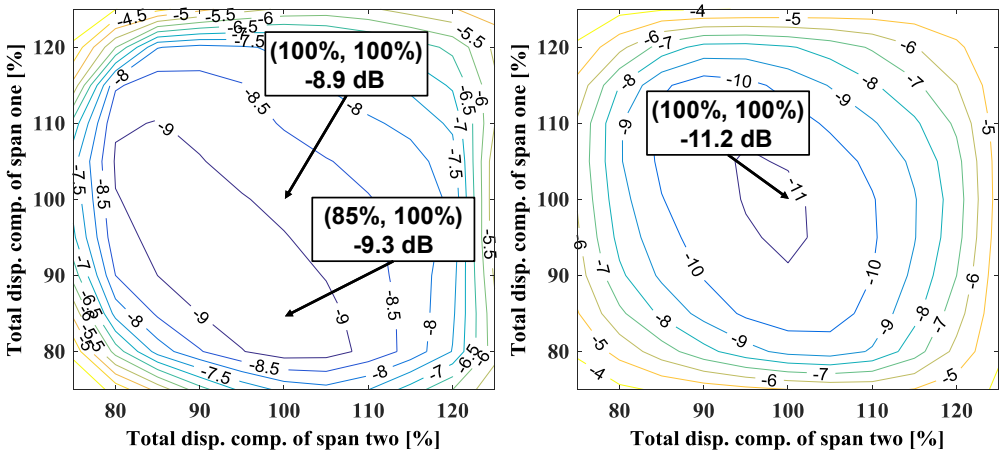

(a) (b)

Fig. 7. Two-span PSA amplified link simulation results at 12 dBm signal launch power showing the EVM performance as a function of total dispersion compensation applied before CS of span 1 and 2 with (a) one span optimized (15%, 15%) and (b) two-span optimized (5%, 35%) dispersion map configurations.

shown. By allowing extra degrees of freedom by different total dispersion compensation values in both spans, the EVM performance can be improved by 0.4 dB, if 15% residual dispersion in span 1 is applied compared to the fully dispersion compensated spans case. In Fig. 7(b) the two-span optimized dispersion map configuration (5%, 35%) is shown with varied total dispersion compensation values. As can be seen, allowing for residual dispersion in the two-span optimized dispersion map case does not improve the EVM performance further. The two-span PSA link with optimized dispersion map shows, however, 1.9 dB better EVM performance than one-span optimized two-span PSA link with residual dispersion in both spans allowed.

5. Long-haul simulations

The optimized two-span PSA link dispersion map (5%, 35%) was applied repeatedly in long-haul transmission simulations and compared with the one-span optimized dispersion map, where the same 15% dispersion pre-compensation was applied in every span. In Fig. 8(a), EVM as a function of transmission distance for two dispersion map scenarios are shown at 9 dBm signal launch power. The two-span optimized case shows 2.1 fold increase in the transmission distance (23 spans) compared to the one-span optimum case (11 spans) at an EVM level of -5 dB. The two-span optimized dispersion map outperforms one-span optimized case after the first span. During the first decade of spans, the EVM fluctuations after the even number of transmitted spans for the two-span optimized case are well observable.

A long-haul transmission comparison at optimal launch power in the presence of amplifier noise with a PSA noise figure of 1 dB [1] is shown in Fig. 8(b). The optimal launch power for the two-span optimized case is 2 dB higher than in the one-span optimized case and the reach increase is 1.5 times, 289 spans compared to 197 spans with single-span optimized case at an EVM level of -5 dB. The results of Figs. 8(a) and 8(b) were also verified with bit error ratio (BER) simulations that show approximately the same distance improvement factors at BER = 10^{-3} for both cases.

Figure 9 shows the constellation diagrams as a comparison of the two dispersion map optimized cases illustrated in Fig. 8(a) at 9 dBm signal launch power and in Fig. 8(b) at optimal signal

Optics EXPRESS

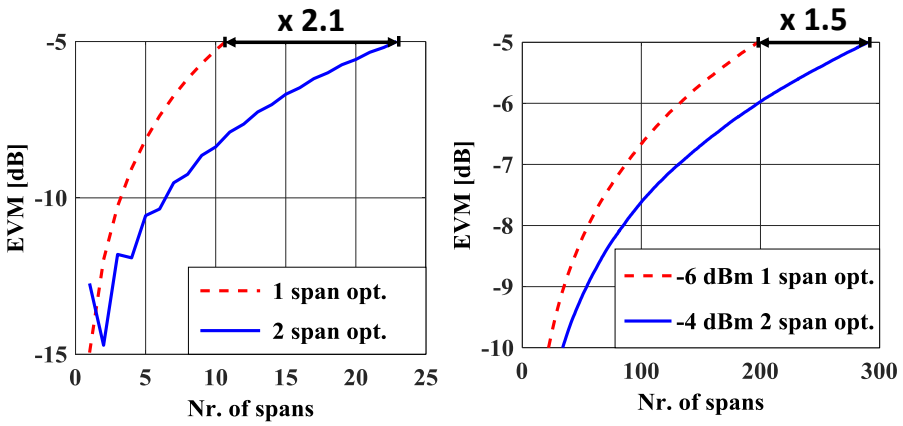

(a) (b)

Fig. 8. Simulation results for long-haul transmission showing EVM as a function of propagated distance in spans, comparing one-span optimized and two-span optimized dispersion maps (a) at 9 dBm signal launch power and (b) at optimal launch power in the presence of amplifier noise.

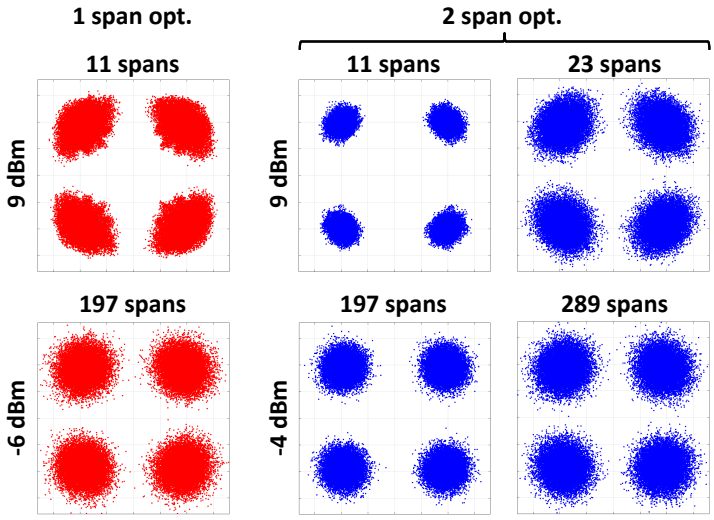

Fig. 9. Constellation diagrams of long-haul PSA transmission link simulations comparing one-span and two-span optimized dispersion maps at 9 dBm signal launch power and at optimal launch powers.

launch powers. The constellations of two optimized dispersion maps in Fig. 9 are compared at transmission reach, where the EVM level is -5 dB. These constellations show similarly that at the same transmission reach, the constellations are less distorted using two-span optimized dispersion map and the reach can be extended up to 2.1 times at 9 dBm signal launch power and up to 1.5 times at optimal signal launch powers to achieve equally distorted contellations compared to the one-span optimized dispersion map in a long-haul transmission link.

Optics EXPRESS

6. Conclusion

The optimized dispersion map configuration for a two-span single-channel 28 GBaud QPSK PSA amplified link was investigated in simulations and verified by an experimental study. Using the same amount of dispersion pre- and post-compensation values for both spans is suboptimal with respect to the efficiency of mitigating nonlinear distortions by span-wise CS. Also the means to optimize dispersion map of a conventional dispersion managed PIA transmission link, do not apply for the dispersion map optimization of the two-span PSA link. Allowing residual dispersion per span does not improve the performance of two-span dispersion map optimized PSA links. Simulation results show that applying two-span optimized dispersion map repeatedly in a long-haul transmission can improve the maximum transmission reach by a factor of 1.5 compared to the one-span dispersion map optimized long-haul PSA amplified transmission.

Funding

Estonian Research Council (PUT1156); European Research Council (ERC) (ERC-2011-AdG-291618 PSOPA).